Met Office

Predictability barriers and diabatic processes

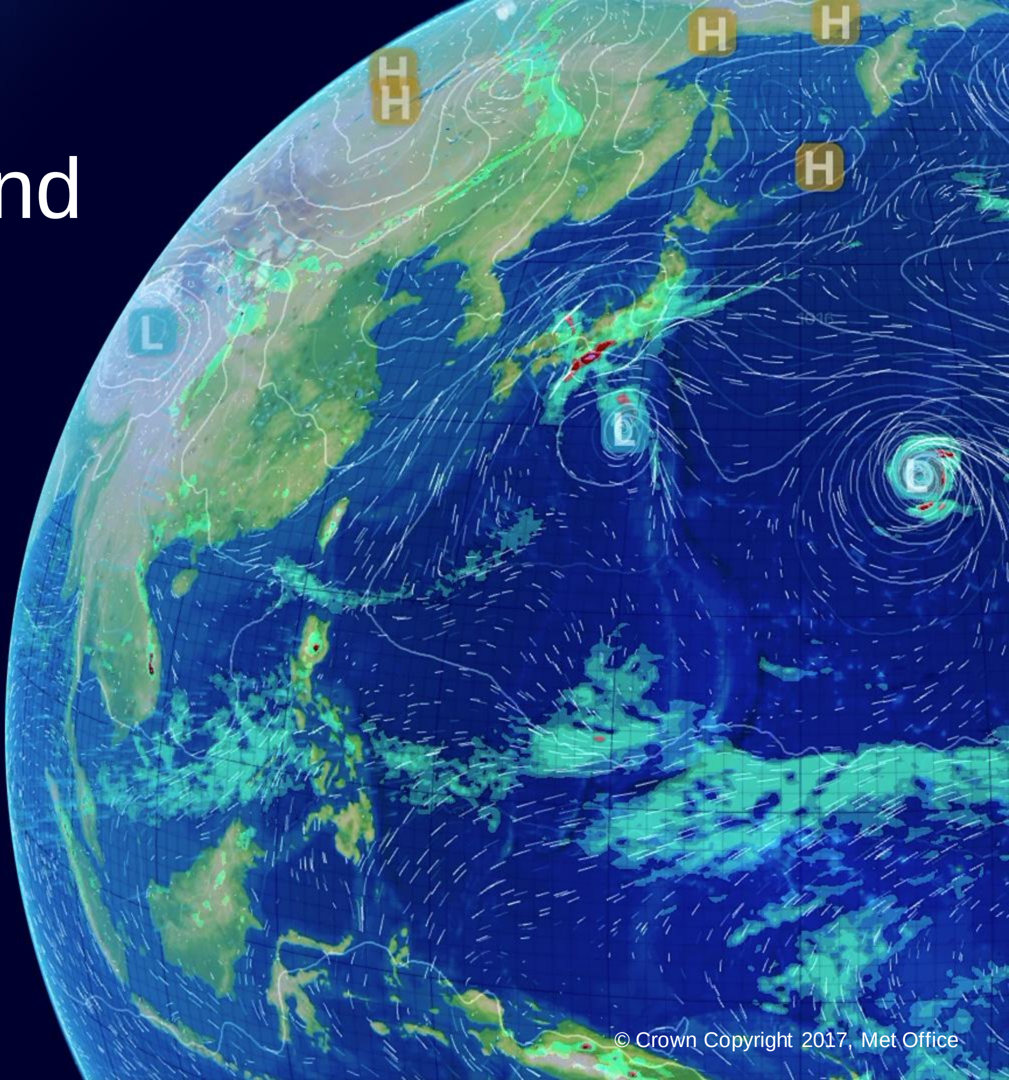

Claudio Sanchez, John Methven, Mike Cullen

NAWDEX workshop

Toulouse, 26/03/2019

Met Office

Outline

- Revisiting predictability barriers from George’s talk last year
- Predictability barriers for UM and EC det. and UM Ensemble during NAWDEX period (15 Sept. to 15 Oct 2016)
- Semi-Geostrophic (SG) inversion model: tracking footprints of diabatic processes
- Results from SG model and diabatic tracers from a pseudo-operational MetUM

Predictability barriers

ACC as function of start and valid time

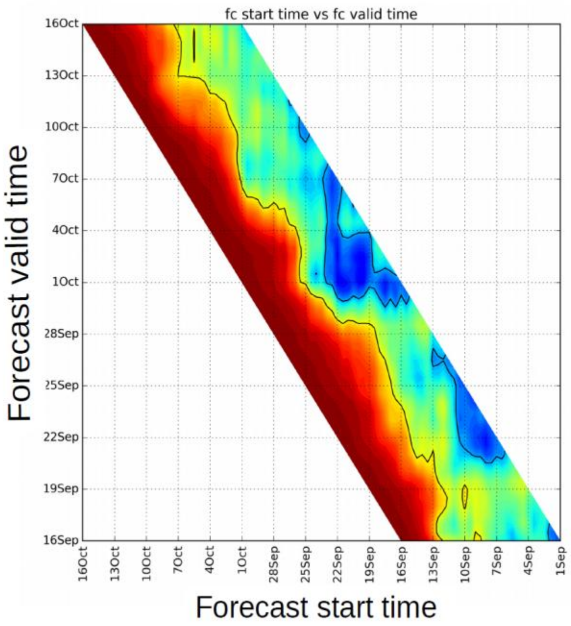

Rate of change of ACC

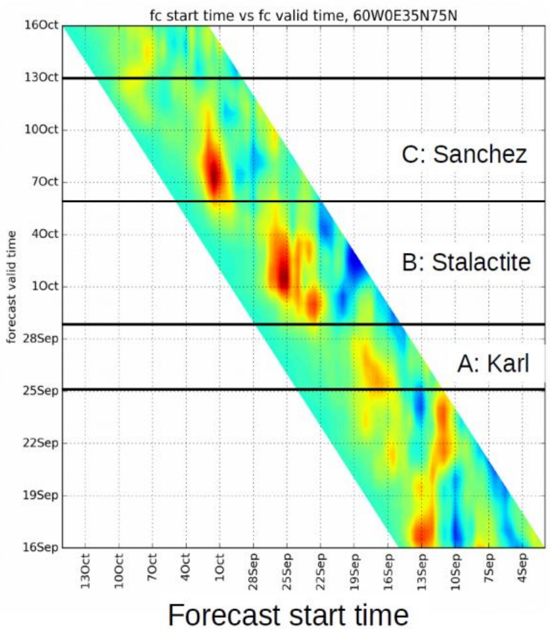

Rate of change of *ACC* for *ECMWF Z500 increases at particular validation times*, defined as *"predictability barriers"*

Craig et al. (2018): Predictability barriers, *NAWDEX 2018 workshop, Munich*

Predictability barriers (2)

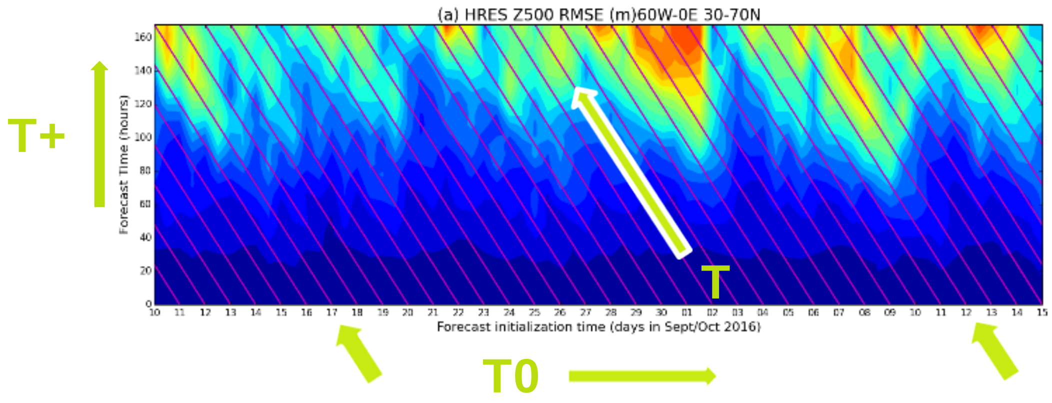

Error T+ profiles for forecasts initialized at 00Z (a) 10 , (b) 11, (c) 12 and (d) 13 9/2016.

Skill drops suddenly around 16th 12Z (T+156, T+132,T+108,T+84)

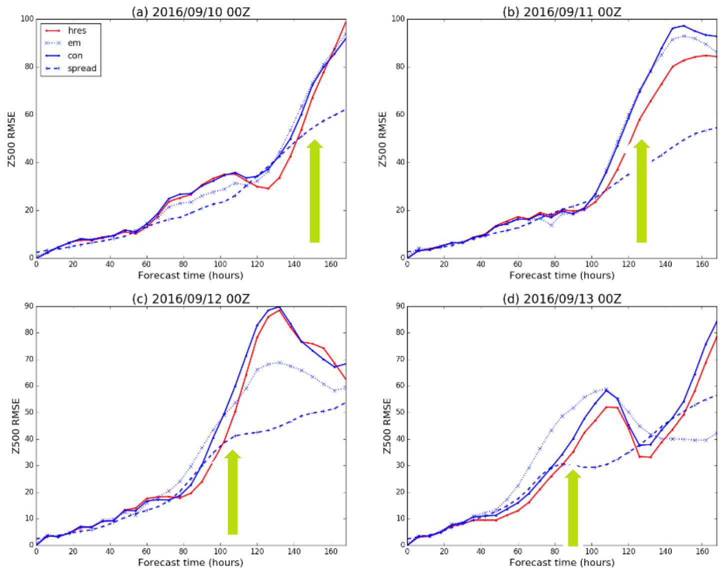

Error in 2D: Init. time 'T0' vs validation time 'T+'

Events that generate larger errors are clear and attributable to particular periods.

Some of the events occur in the same day regardless of the forecasts time (e.g. 17/09 or 12/10) [Follow 'validation time' diagonal lines]

Met Office

Predictability barriers (3)

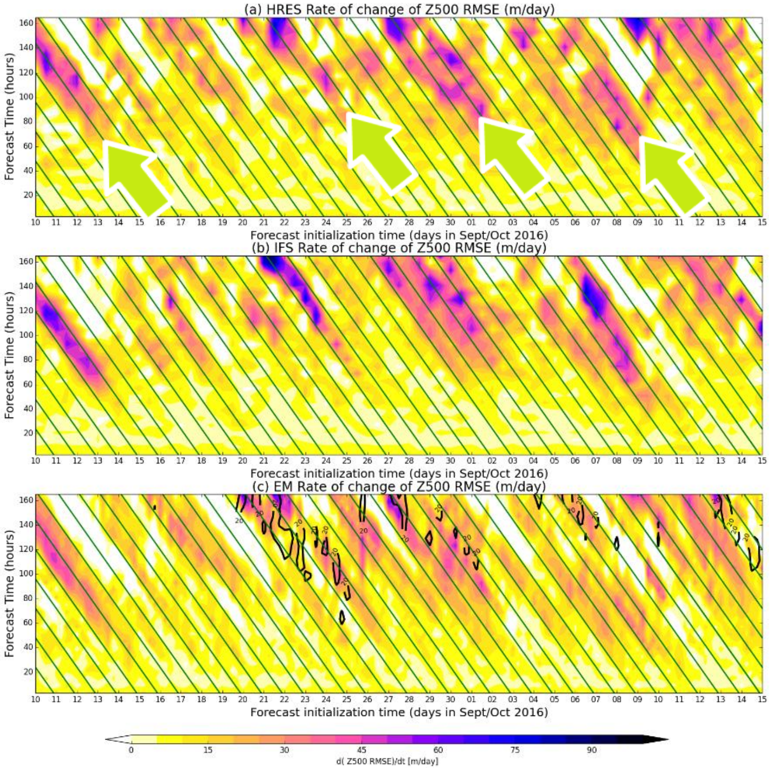

Doing the error tendency (∂ 'error' / ∂ 'T+'):

Clear signal of forecast skill drop for given days (16th + 29th Sept, 5th + 12th Oct).

Predictability barriers!!

Σ validation time: Spread insensitive to barriers!

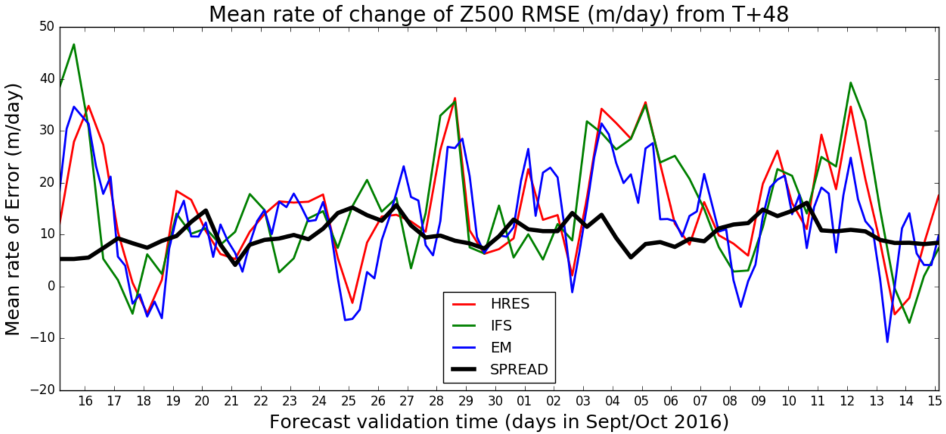

Met Office

NAWDEX and SG results

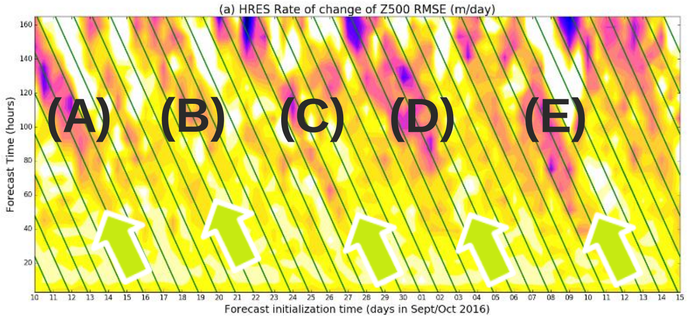

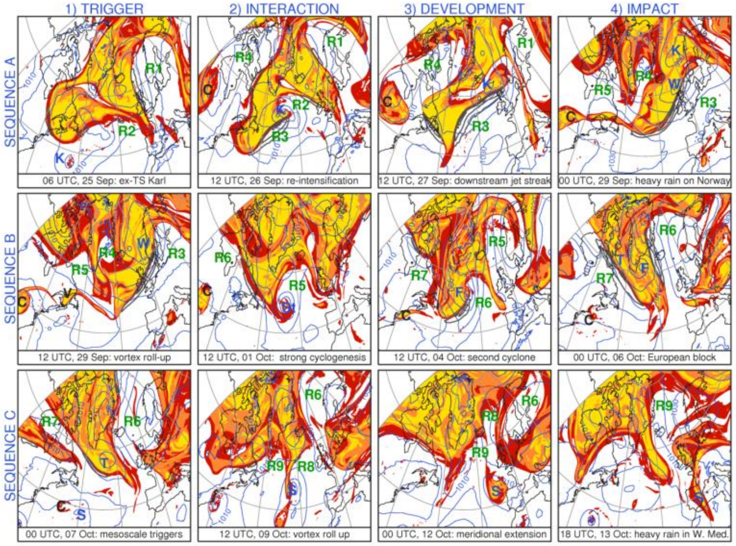

(A): 16th-18th Sept. *Ex-TC Ian*. IOP 1

(B): 22nd-23th Sept. *Vladiana* IOP 4

(C): 28-29th Sept. *Walpurga* + *Ex-TC Karl*. IOP 5

SEQUENCE A

(D): 4th-6th Oct. Downstream effects of *Stalactite cyclone* + blocking development. IOP 6-7

SEQUENCE B

(E): 11-13th Oct. PV cut off *Sanchez* + tropopause ridge *Thor*. IOP 9-10

SEQUENCE C

[Left] NAWDEX golden cases (aka Sequences)
Fig 6. Schaffler et al. 2018

Linking predictability barriers to diabatic processes …

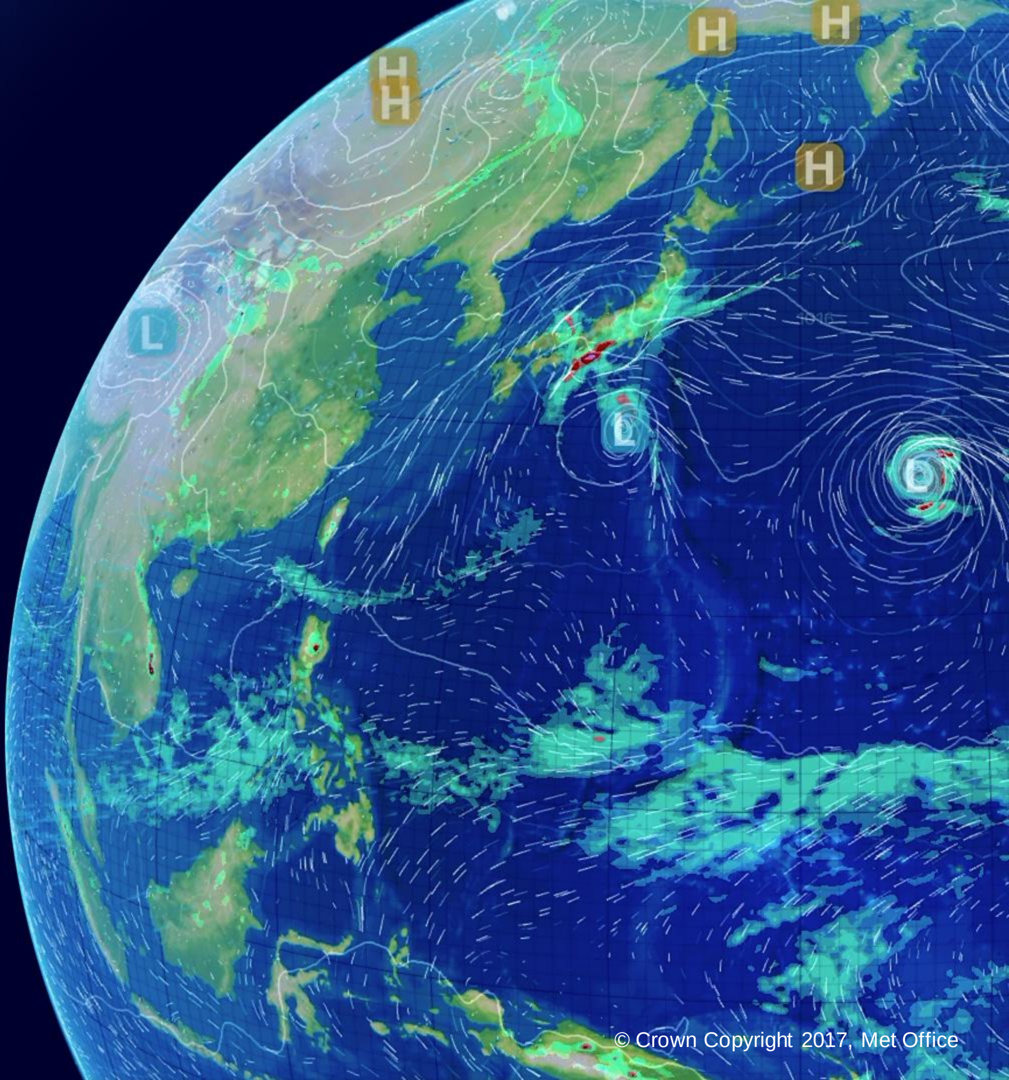

Met Office Semi-Geostrophic (SG) Inversion Model

UM eqs:

$$\frac{D\mathbf{u}}{Dt} + c_{pd}\theta_v \nabla \pi + 2\Omega \times \mathbf{u} = \mathbf{g} + \frac{\partial}{\partial r}\left(K_m \frac{\partial \mathbf{u}_h}{\partial r}\right) + S_{\mathbf{u}},$$

$$\frac{D\theta_{vd}}{Dt} = S_{\theta_{vd}},$$

+

SG eq:

$$c_{pd}\theta_v \nabla_h \pi - (f v_e, -f u_e) = \frac{\partial}{\partial r}\left(K_m \frac{\partial \mathbf{u}_e}{\partial r}\right)$$

$$c_{pd}\theta_v \frac{\partial \pi}{\partial r} = -g.$$

Π: Exner pressure

K_m: BL diffusion coef.

S: Source terms

v_e: Geotriptic wind

$$\mathbf{BQ}'\begin{pmatrix} u - u_e \\ v - v_e \\ w \end{pmatrix} + c_{pd}\theta_v \frac{\partial}{\partial t}\begin{pmatrix} \frac{1}{r\cos\phi}\left(\frac{\partial \pi}{\partial \lambda} - \frac{\partial \pi}{\partial r}\frac{\partial r}{\partial \lambda}\right) \\ \frac{1}{r}\left(\frac{\partial \pi}{\partial \phi} - \frac{\partial \pi}{\partial r}\frac{\partial r}{\partial \phi}\right) \\ \frac{\partial \pi}{\partial r} \end{pmatrix} = \mathbf{BH}'$$

$$\mathbf{H}' = \begin{pmatrix} -(\mathbf{u}_e\theta_v)\cdot\nabla\left(\frac{v_e}{\theta_v}\right) + S_v - \frac{v_e S_{\theta_v}}{\theta_v} \\ (\mathbf{u}_e\theta_v)\cdot\nabla\left(\frac{u_e}{\theta_v}\right) - S_u + \frac{u_e S_{\theta_v}}{\theta_v} \\ -\mathbf{u}_e\cdot\nabla\theta_v + S_{\theta_v} \end{pmatrix}$$

SG model able to solve pressure tendency (dπ/dt), ageostrophic wind ($v - v_e$) and balanced vertical wind (w).

Source Matrix H': linear comb. of geostrophic term plus friction and diabatic sources

More info in ***Cullen (2018):*** *The Use of Semigeostrophic Theory to Diagnose the Behaviour of an Atmospheric GCM, fluids 3,72*

SG and predictability barriers

SG model integrated for one hour from pseudo-operational Met-UM (17km) at T+1,3,5 D. Only diabatic sources (S_θ) are considered.

$$-v_{ag}(diab) \cdot \nabla q$$

Ageostrophic advection of PV shows areas where there are cross-tropopause and ridge building action

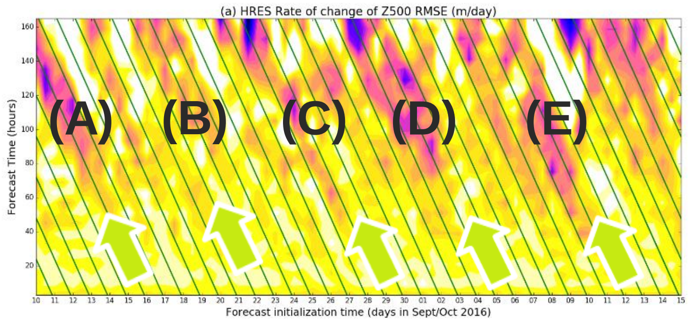

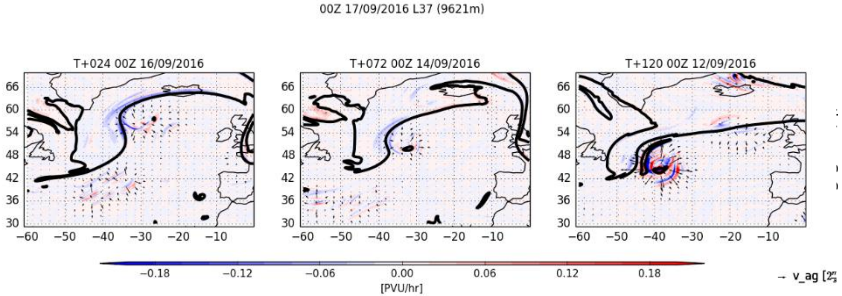

[Top]: v_ag (diab) grad(q) for 17th 00Z Sept. Ridge building delayed in longer forecasts

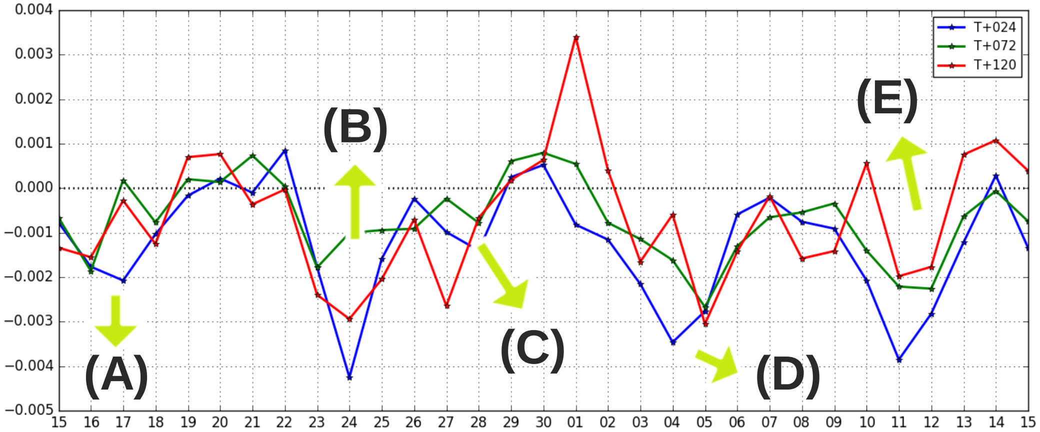

[Top]: v_ag (diab) grad(q) averaged over the predictability barrier domain (60-0E, 30-70N). *Dims: PVU/hr*

Semi-Geostrophic Inversion Model

(Ian: 16 12Z)

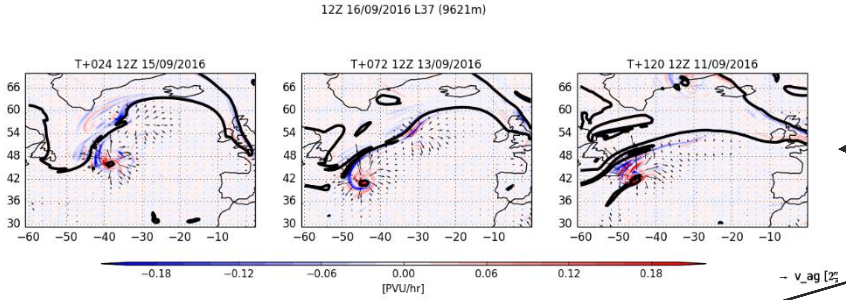

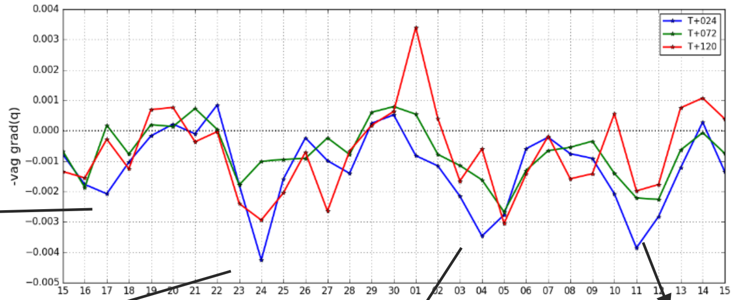

(Sanchez. 10 00Z)

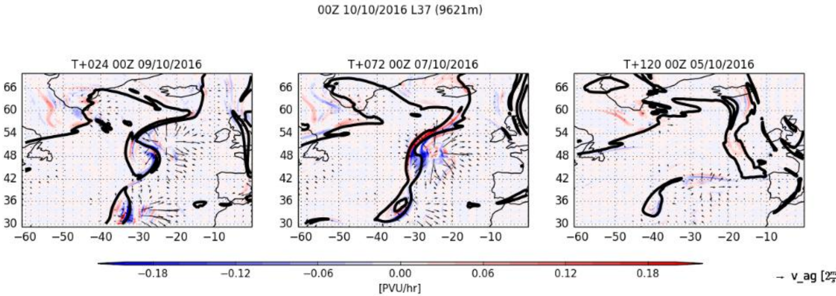

(Vladiana: 24 00Z)

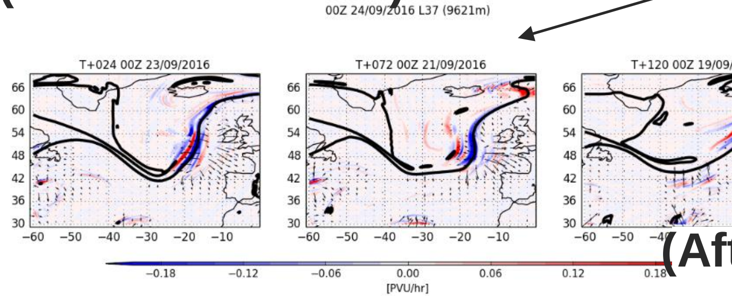

(After St. 5 00Z)

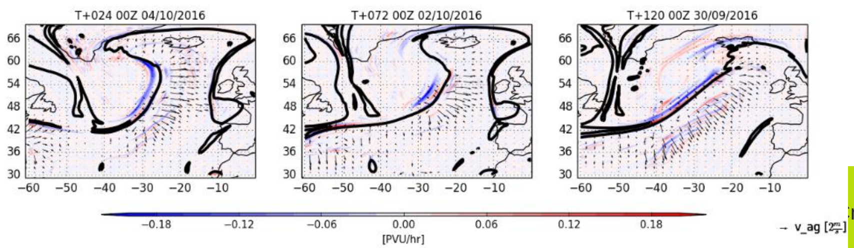

Ex-TC IAN (IOP1)

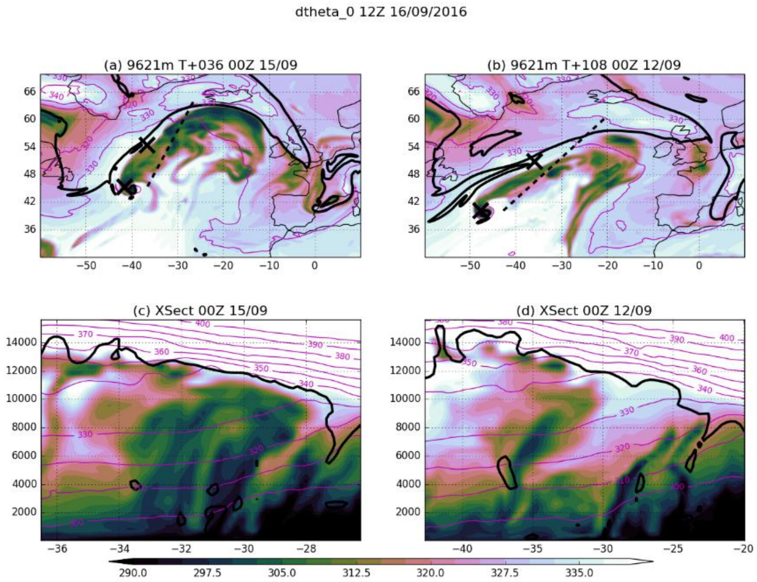

[Top] 'advection only dθ' tracer on 12Z 16th for (a,c) 00Z 15th (b,d) 00Z 12th forecast. (c,d) Cross section on dashed line in (a,b). X: Pos of Ian and merged cyclone. Tracer initialized at 00Z 15th

Longer forecast fail to merge, important ascent and heating from LS-rain over ridge

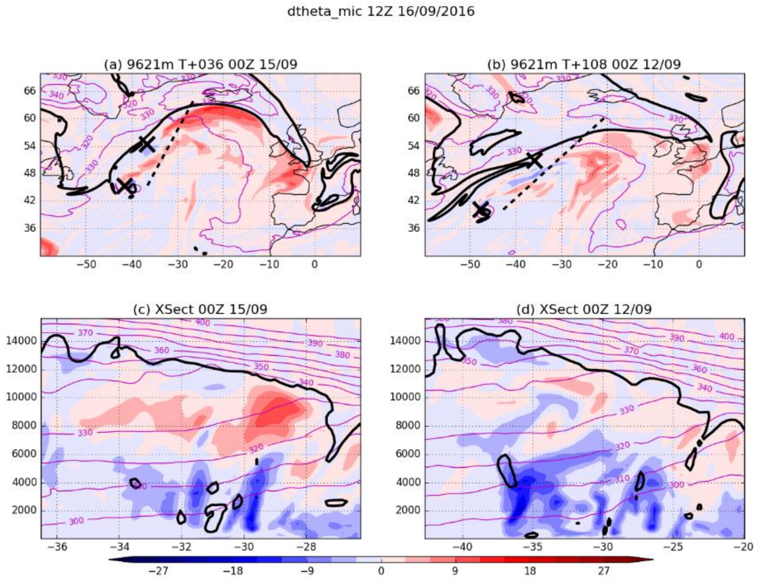

[Top] Same as left, but for $d\theta_{LS}$.

After stalactite (IOP6?)

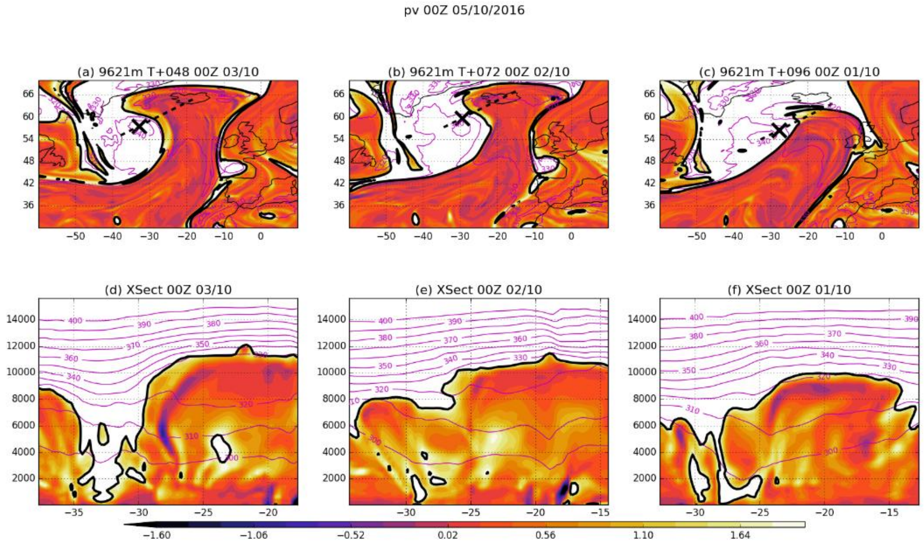

Delay in ridge building, strong negative PV filament associated to LS rain process

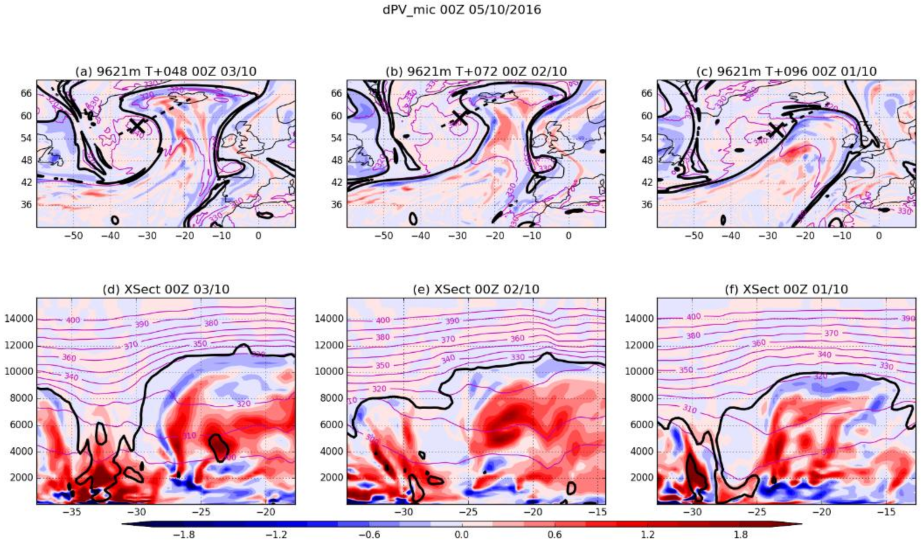

[Top]: PV on 00Z 5th in different forecasts initialized at 00Z 3rd, 2nd and 1st . X shows the position of the stalactite's upstream cyclone.

[Right]: same layout for dPV_{LS} tracer (initialized at 00Z 3rd).

Met Office

Conclusions

- Predictability barriers coincide with important IOP NAWDEX cases (Ian, Karl, Stalactite, Sanchez). Both EC and UM struggle
- UM EPS fail to capture rapid increase of model error
- Semi Geostrophic inversion model provides a neat way to convey the influence of diabatic processes in the flow ("diabatic ageostrophic advection" of PV $-v_{ag}(diab) \cdot \nabla q$)
- Peaks of diabatic ageostrophic advection coincide with predictability barriers, less advection is produced in longer forecasts

Thanks for your attention!

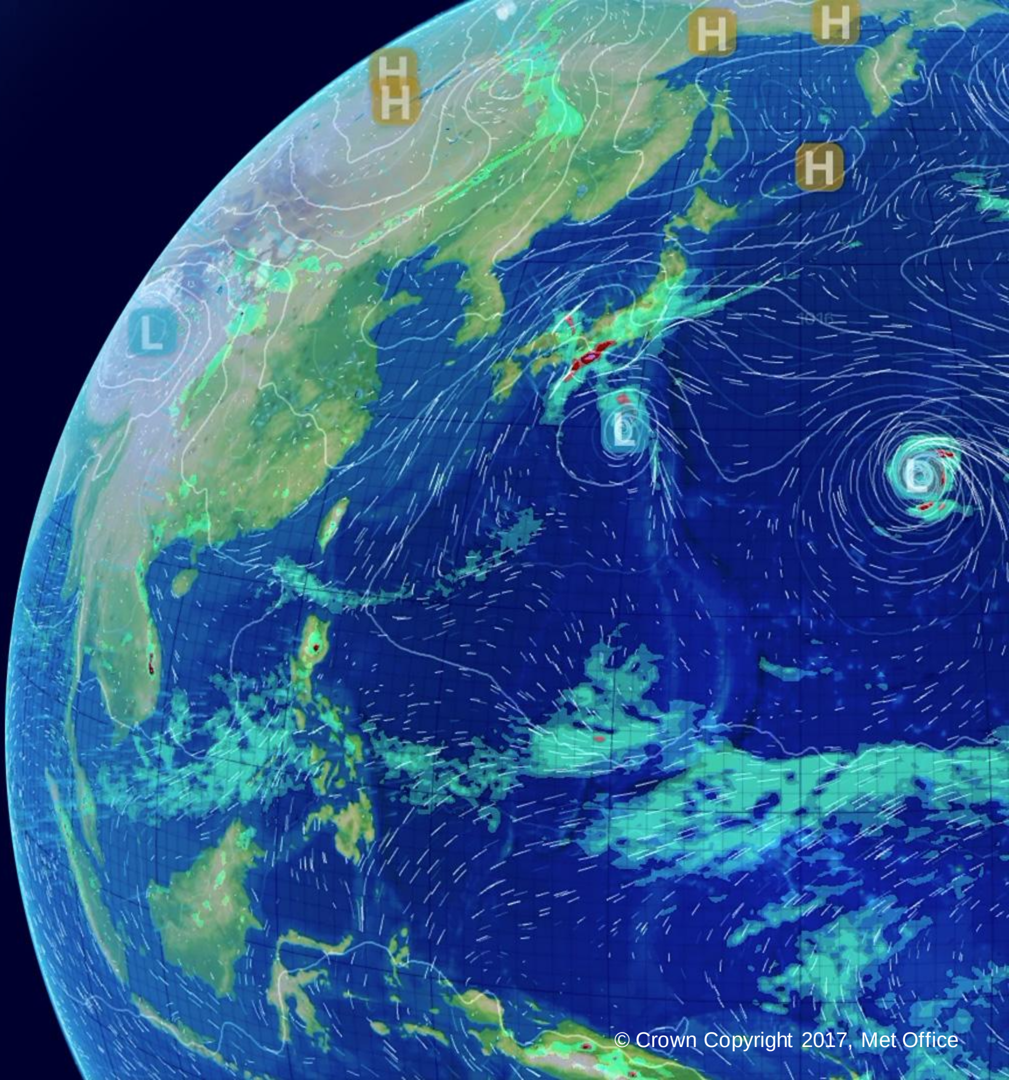

Semi-Geostrophic Inversion Model

$$\mathbf{B}\mathbf{Q}'\begin{pmatrix} u-u_e \\ v-v_e \\ w \end{pmatrix} + c_{pd}\theta_v\frac{\partial}{\partial t}\begin{pmatrix} \frac{1}{r\cos\phi}\left(\frac{\partial\pi}{\partial\lambda}-\frac{\partial\pi}{\partial r}\frac{\partial r}{\partial\lambda}\right) \\ \frac{1}{r}\left(\frac{\partial\pi}{\partial\phi}-\frac{\partial\pi}{\partial r}\frac{\partial r}{\partial\phi}\right) \\ \frac{\partial\pi}{\partial r} \end{pmatrix} = \mathbf{B}\mathbf{H}'$$

Where

$$\mathbf{B} = \begin{pmatrix} f & -\frac{\partial}{\partial r}\left(K_m\frac{\partial}{\partial r}\right) & 0 \\ \frac{\partial}{\partial r}\left(K_m\frac{\partial}{\partial r}\right) & f & 0 \\ 0 & 0 & g/\theta_v \end{pmatrix}$$

$$\mathbf{Q}' = \begin{pmatrix} f+\frac{\theta_v}{r\cos\phi}\frac{\partial}{\partial\lambda}\left(\frac{v_e}{\theta_v}\right)+\frac{u_e\tan\phi}{r} & \frac{\theta_v}{r}\frac{\partial}{\partial\phi}\left(\frac{v_e}{\theta_v}\right)+\frac{\partial}{\partial r}\left(K_m\frac{\partial}{\partial r}\right) & \theta_v\frac{\partial}{\partial r}\left(\frac{v_e}{\theta_v}\right) \\ -\frac{\theta_v}{r\cos\phi}\frac{\partial}{\partial\lambda}\left(\frac{u_e}{\theta_v}\right)+\frac{v_e\tan\phi}{r}-\frac{\partial}{\partial r}\left(K_m\frac{\partial}{\partial r}\right) & f-\frac{\theta_v}{r}\frac{\partial}{\partial\phi}\left(\frac{u_e}{\theta_v}\right) & -\theta_v\frac{\partial}{\partial r}\left(\frac{u_e}{\theta_v}\right) \\ \frac{1}{r\cos\phi}\frac{\partial\theta_v}{\partial\lambda} & \frac{1}{r}\frac{\partial\theta_v}{\partial\phi} & \frac{\partial\theta_v}{\partial r} \end{pmatrix}$$

Elliptic equation for

$\partial\pi/\partial t$

$$\frac{\kappa_d-1}{\kappa_d}\frac{\rho_d}{\pi}r^2\frac{\partial r}{\partial\eta}\frac{\partial\pi}{\partial t}+r^2\frac{\partial r}{\partial\eta}\frac{\rho_d c_{pd}\theta_v^2}{g\theta_{vd}}\frac{\partial}{\partial t}\left(\frac{1}{(1+\mu)}\frac{\partial\pi}{\partial r}\right)+\nabla\cdot\left(r^2\rho_d c_{pd}\theta_v\frac{\partial r}{\partial\eta}\mathbf{R}\mathbf{P}^{-1}\frac{\partial}{\partial t}\left(\nabla_r\pi\right)\right)=$$
$$\nabla\cdot\left(r^2\rho_d\frac{\partial r}{\partial\eta}\mathbf{R}\mathbf{P}^{-1}\mathbf{G}\right)+\frac{1}{\cos\phi}\left(\frac{\partial}{\partial\lambda}\left(r\rho_d u_e\frac{\partial r}{\partial\eta}\right)+\frac{\partial}{\partial\phi}\left(r\rho_d v_e\cos\phi\frac{\partial r}{\partial\eta}\right)\right).$$

Vertical velocity can be deduced using the S-G omega equation.

Its form in momentum coordinates (Hoskins & Draghici, 1977) is:

$$\nabla_X^2\left(\frac{g\rho_r}{\theta_0 f_0}q_g w^*\right)+f_0^2\frac{\partial^2 w*}{\partial Z^2}=\boxed{2\nabla_X.\mathbf{Q}}+\boxed{\nabla_X^2 H}\qquad H=\alpha w^*\ ,\qquad \hat{Z}=\frac{N_0}{f_0}Z$$

Geostrophic forcing

Diabatic forcing (H=heating)

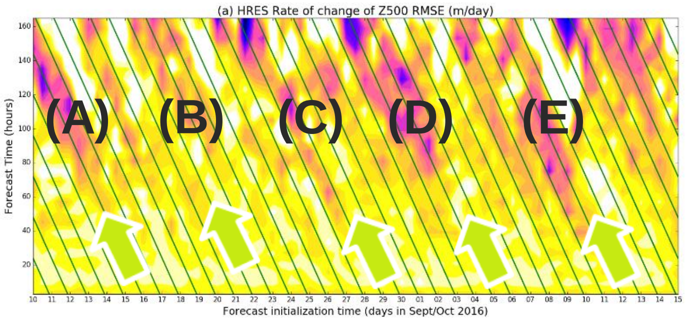
(a) HRES Rate of change of Z500 RMSE (m/day)
Forecast Time (hours)
Forecast initialization time (days in Sept/Oct 2016)
(A)
(B)
(C)
(D)
(E)

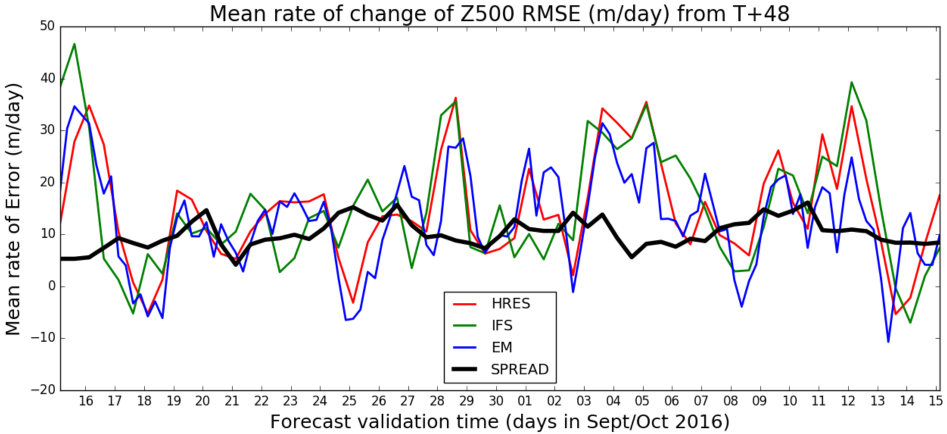
Mean rate of change of Z500 RMSE (m/day) from T+48
Mean rate of Error (m/day)
Forecast validation time (days in Sept/Oct 2016)
HRES
IFS
EM
SPREAD

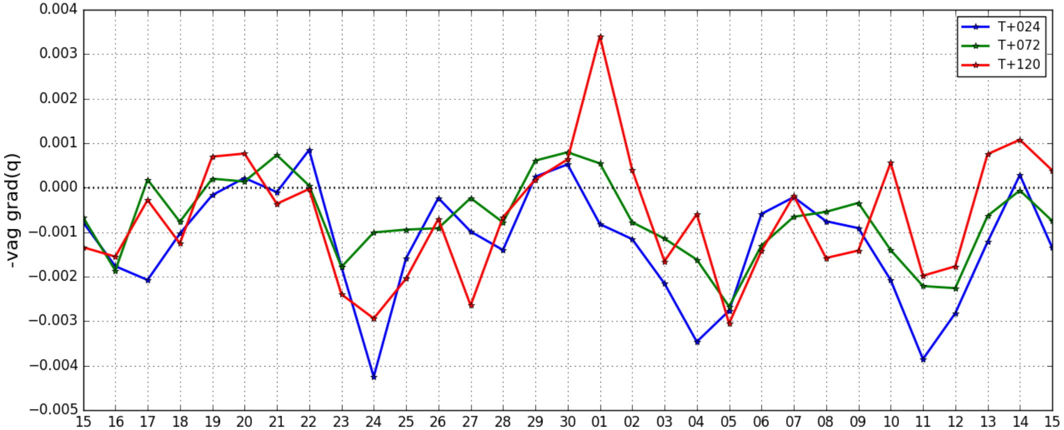
-vag grad(q)
T+024
T+072
T+120